Microstructure of diffusional zirconia–titanium and zirconia–(Ti–6 wt% Al–4 wt% V) alloy joints

R. N. CORREIA, J. V. EMILIANO*
Departmento de Engenharia Cerâmica e do Vidro, University of Aveiro, 3810 Aveiro, Portugal

P. MORETTO
Institute of Advanced Materials, Joint Research Centre CEC, 1755 ZG Petten, The Netherlands

Zirconia–titanium and zirconia–titanium alloy joints were made by diffusion bonding under an inert atmosphere at temperatures in the 1162–1494 °C range. To inhibit the strong oxygen uptake by the titanium member a platinum insert was alternatively used. The microstructures and elemental profiles across the joints were investigated by scanning electron microscopy imaging and energy-dispersive spectroscopy or wavelength-dispersive spectroscopy microanalysis. It was found that direct ZrO_2–Ti joining produces oxygen saturation in the Ti member and the formation of $(Ti, Zr)_2O$ at the interface. ZrO_2/Pt/Ti joints present a complex layer sequence which at lower temperatures can be described on the basis of the Pt–Ti binary, except near the ceramic where a (Pt, Zr)-rich layer forms; at higher temperatures these joints develop an oxide layer of composition Ti_2O_3, this oxide probably resulting from local decomposition of the ceramic and reaction of oxygen with the incoming titanium. When Ti is replaced by the Ti–6 wt% Al–4 wt% V alloy in joints where Pt is present, the main consequences are the presence of liquid at lower joining temperatures and the earlier development of the oxide layer, now of nominal composition TiO. In all Pt-containing joints a phase of nominal composition Ti_3Pt_2 forms; it is advanced that this may be an equilibrium phase not predicted by the Pt–Ti diagrams available. All joints are weak, the fracture path running through the metal in the case of direct ZrO_2–Ti joints and through the interface between the ceramic and the (Pt, Zr)-rich layer in joints where Pt is present.

1. Introduction

Tetragonal zirconia polycrystal (TZP) is a monolithic ceramic with outstanding flexural strength and fracture toughness. Titanium alloys, particularly Ti–6 wt% Al–4 wt% V, are structural materials for aerospace and biomedical applications. From the biomedical point of view, radioactive element-free zirconia ceramic is a biocompatible material. Coupling of the two types of material for purposes where the specific properties of a ceramic should coexist with those of a metal looks promising. An example is the encapsulation of intelligent sensing devices where the ceramic would act as a radio-frequency window.

Joining of TZP and titanium alloys presents difficulties owing to the high oxygen affinity of the metal, although the similarity of the expansion coefficients of both members (at moderate temperatures as follows: TZP, 9.6 MK^{-1}; Ti, 9 MK^{-1}; Ti–6 wt% Al–4 wt% V, 9.4 MK^{-1}) and the moderately high Young's modulus of TZP (200 GPa, as against 110 GPa for annealed Ti and alloy) are attractive features in potential joints. Previous work [1] has shown that ZrO_2–Ti brazing at 900 °C using Cusil ABA® results in strong joints (four-point bending strengths of 400–450 MPa). Since zirconium and titanium are mutually and completely soluble [2], diffusion bonding would be appealing, since it does not introduce foreign elements of doubtful biocompatibility, such as copper in brazing alloys. In this paper, attempts of diffusion bonding TZP to Ti and to Ti–6 wt% Al–4 wt% V either directly or with the interposition of a platinum interlayer are described, together with the microstructural and compositional characterization of the joints thus formed.

2. Experimental procedure

ZrO_2–3 mol% Y_2O_3 powders (Tosoh TZ-3YB) were sintered to produce fully dense TZP ceramic specimens. These were cut into discs 10 mm in diameter and 5 mm high, whose faying surfaces have been polished in several abrasives, ending with a suspension of colloidal silica. Titanium sheet (purity, 99.5%; Goodfellow) and Ti–6 wt% Al–4 wt% V sheet (purity, 99.5%; DTG) 1 mm thick were cut into 10 mm × 10 mm squares, chemically treated in an aqueous solution of 15 vol% HNO_3 + 5 vol% HF to remove the

*Present address: Centro de Tecnologia em Cerâmica, 88802-330 Criciúma/SC, Brazil.

0022–2461

oxide surface layer, rinsed and ultrasonically cleaned in acetone. Platinum foil (Engelhard) 25 μm thick was also cut to size and ultrasonically cleaned in acetone.

ZrO_2/Ti/ZrO_2, ZrO_2/Pt/Ti/ZrO_2 and ZrO_2/Pt/(Ti–6 wt% Al–4 wt% V)/ZrO_2 blocks were joined at temperatures of 1162, 1245, 1328 and 1494 °C, conventionally chosen to correspond to 0.7, 0.75, 0.8 and 0.9 of the melting temperature of titanium, under a continuous flow of argon and a 5 MPa mechanically applied pressure, for times of 15–180 min. The argon (Air Liquide N50) was nominally 99.999% pure, with specified maximum 2 ppm free O_2 and 3 ppm H_2O, the other main impurities being hydrocarbons.

After cutting and polishing, the elemental concentration profiles across the joints were determined by electron probe microanalysis (EPMA)–wavelength-dispersive spectroscopy (WDS), using Kα characteristic lines for O, Ti, Y, Al and V and Lα lines for Zr and Pt. High-purity metal standards were used for V, Zr and Pt, a stoichiometric standard of TiO_2 for O and Ti, and a yttrium aluminium garnet-containing standard ($Y_3Al_5O_{12} + Y_2O_3 + Al_2O_3$) for Y and Al. Concentration profiles were determined at accelerating voltages between 10 and 20 kV (the latter is necessary for Pt analysis in the presence of Zr). In many instances, concentrations in profiles were checked by averaged point analysis. During scans the probe diameter was usually 1 μm, but 0.3 μm probe scans were also used to increase the resolution in the analysis of the thinnest layers. Joints were observed under scanning electron microscopy (SEM) and occasionally analysed by energy-dispersive spectroscopy (EDS), namely, for determination of oxygen in TiO_x layers, using high-purity titanium as a standard. The experimental errors associated with the measurements are ± 5% for EDS and ± 2% for WDS.

In a particular case the interfacial region exposed after fracture has been analysed by X-ray diffraction using Cu Kα radiation at a constant 1° glancing angle, the outgoing radiation being monochromated by a curved graphite crystal.

3. Results and discussion

3.1. Tetragonal zirconia polycrystal/Ti system

Interfaces with enough strength for ceramographic preparation of cross-sections were obtained only at high temperatures: 1328 °C (15–180 min) and 1494 °C (1–180 min). The microstructure of the interfacial region consists of two layers, of increasing thickness with temperature and time (Fig. 1). The layer a adjacent to the Ti metal is apparently of *a* single-phase nature, whereas the layer *b* adjacent to the ceramic has a duplex structure, consisting of a matrix, continuous with the previous layer, and a dispersed phase; the composition of both phases in *b* could not be quantified because of their smallness compared with the spatial resolution of the probe. Layers *a* and *b* are both electrically conductive.

These joints are characterized by extensive blackening of the ceramic, indicating oxygen loss. However, no quantifiable reduction has been detected by WDS. The elemental atomic concentration profiles are independent of joining temperature and time and are exemplified in Fig. 2. The O concentration [O] (the brackets [ ] indicating concentration) in layer b decreases towards the metallic member in an almost symmetrical way as the increase in [Ti], whereas [Zr] shows no definite trend. Across *a*, [Zr] and [Ti] vary drastically. It is noted that [O] in *a* is the same as in Ti (32 at%, which is near the reported solubility limit in Ti at moderate temperatures [3]). It is also noted that, in spite of the well-known total solid solubility of Zr in pure Ti, no Zr is detected in the O-saturated Ti.

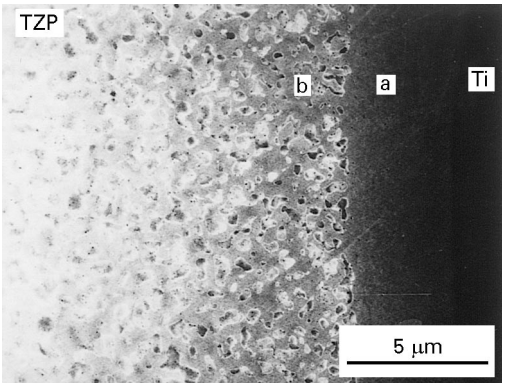

Figure 1 Microstructure of a ZrO_2–Ti joint (1494 °C; 180 min).

In layer *a* the overall composition can be assigned to (Ti, Zr)$_2$O. Detailed profiles using a 0.3 μm probe indicate a [Ti]/[Zr] ratio in the layer increasing from 1 near the ceramic to 2 near the metal. The presence of this distinct layer of oxide, with the same oxygen content as the titanium member, means that oxygen solubility in the metal is decreased when zirconium is also present. Small-incidence-angle X-ray diffraction on a carefully prepared fracture surface, from which the major part of the metal had been removed, indeed gave a best fit for Ti_2O. It should be noted that the presence of this oxide is not predicted by available data for the Ti–ZrO_2 pseudobinary [4], which indicates $(Ti, Zr)_3O$ as the stable oxide in equilibrium with α-Ti(Zr, O) in the [Ti] range 75–64 at%.

The fact that in the duplex layer *b* the concentrations merge smoothly with those found in the bulk of the zirconia and the reported continuity of the matrix phase with layer *a* leads to the possibility that *b* is formed by $(Zr, Ti)O_2 + (Zr, Ti)_2O$. Again, this coexistence of phases is not consistent with previous data [4].

The fracture strength of the joints is negligible, and the fracture path runs through the embrittled metal, rather than along the interface. This embrittlement is accompanied by a drastic increase in the Vickers hardness resulting from oxygen dissolution in titanium 736 ± 71 HV after joining, compared with about 60 HV in the pure annealed metal), together with exaggerated grain growth (two orders of magnitude) at the joining temperatures.

3.2. Tetragonal zirconia polycrystal/Pt/Ti system

In this system it was found that for lower temperatures and shorter times the joints have not survived cutting,

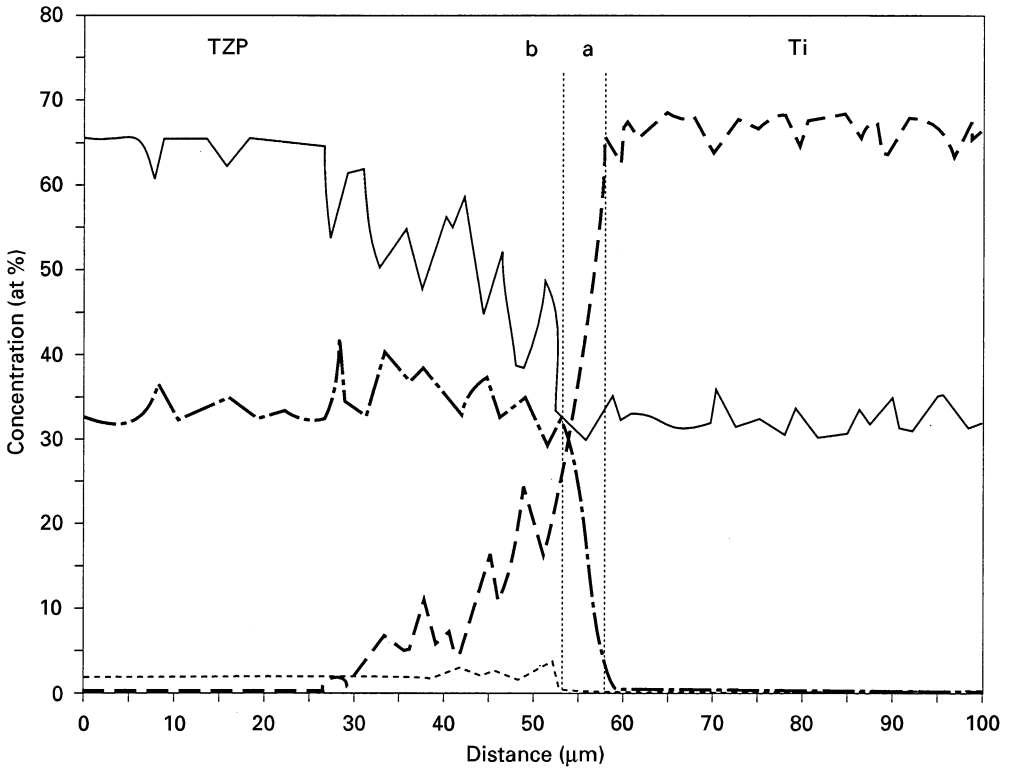

Figure 2 EPMA profiles in a ZrO_2–Ti joint (1494 °C; 180 min). Experimental points are not shown for clarity. (——), O; (– – –), Ti; (- - - -), Y; (— - —), Zr.

the separation invariably occurring at the ZrO_2–Pt interface. Bonded specimens present three types of microstructure.

3.2.1. Joints at subsolidus temperatures

For specimens joined at 1162 °C and 1245 °C, i.e., below the solidus of the Ti–Pt binary system, the interlayers develop in the same sequence, irrespective of time (within the investigated range 15–180 min). A typical microstructure is shown in Fig. 3, with layers labelled from *a* to *g* and Fig. 4 represents the EPMA elemental profiles which are common to all joints, with the exception of some concentration variations in the layers nearer to the ceramic. The virtual absence of oxygen is evident in all layers but *a* and *g*, whereas the concentration of zirconium is less than 5 at% except in *a*. These findings enable us to describe most of the compositions on the basis of the Ti–Pt binary [5], taking into account, whenever needed, that Zr and Ti are likely to be mutually replaceable in a given phase. Layer *a* cannot be described in this way, since it is a Pt-rich phase with Zr and Ti. Pt can dissolve up to 20 at% Zr at low temperatures [6] and 10 at% Ti above 1100 °C, although at lower temperatures the solubility of Ti is probably less [5]. It is thus hypothesized that *a* is a Pt(Zr, Ti) solid solution.

Layer *b* shows a plateau corresponding to the approximate composition (Ti, Zr) Pt_3. It is not certain that $TiPt_3$ or $ZrPt_3$ exists, but in the Ti–Pt diagram [5] the Ti-rich end of the so-called γ-phase lies very close to the composition $TiPt_3$, so that *b* could be either (Ti, Zr) Pt_3 or γ with some dissolved Zr.

The profile of *c* represents a transition between the compositional plateaux of *b* and *d*. Excluding the extreme measurements, which may be affected by adjacent layers, the composition of *c* approaches that of the probable Ti_3Pt_5 intermetallic, so that the composition $(Ti, Zr)_3Pt_5$ is tentatively assigned to this layer. The composition of layer *d* can be ascribed to (Ti, Zr) Pt, whereas the composition of *f* corresponds to Ti_3Pt.

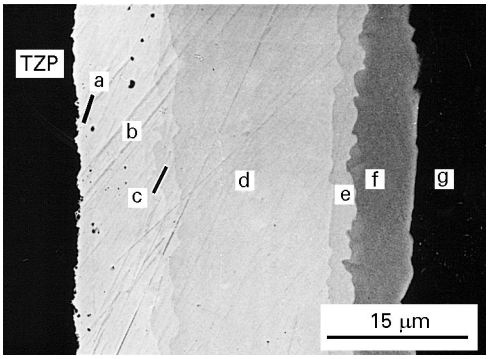

Figure 3 Microstructure of a ZrO_2/Pt/Ti joint (1162 °C; 120 min). The duplex character of layer *g* is not evident owing to contrast effects.

The layer *e*, between layers *d* and *f*, shows a steep compositional profile. When the limiting measured compositons are discarded, the average composition is found to lie within the range $Ti_{1.27}Pt$ and $Ti_{1.43}Pt$. A higher-resolution line scan of three analysis points per micrometre showed a plateau 1.5 μm wide corresponding to $Ti_{1.44}Pt$ (Fig. 5). Also, all the microstructural evidence points towards a single-phase character. Such an intermetallic, hereafter called "Ti_3Pt_2" is not predicted in the Ti–Pt equilibrium diagram. It should be noted that this layer appears in all joints, regardless of temperature and joining time.

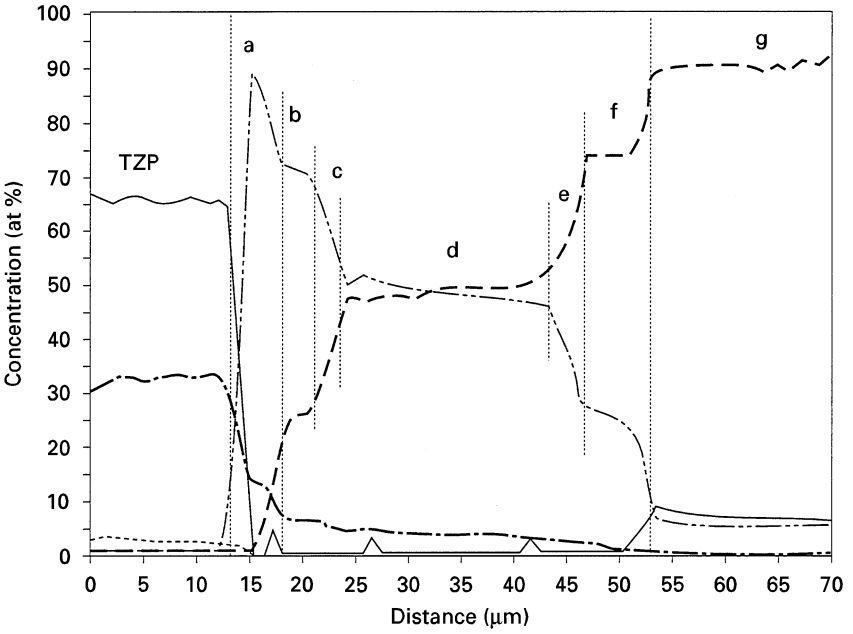

Figure 4 EPMA profiles in a ZrO_2/Pt/Ti joint (1162 °C; 180 min). (——), O; (– – –), Ti; (— - —), Zr; (— - - —), Pt; (- - - - -), Y.

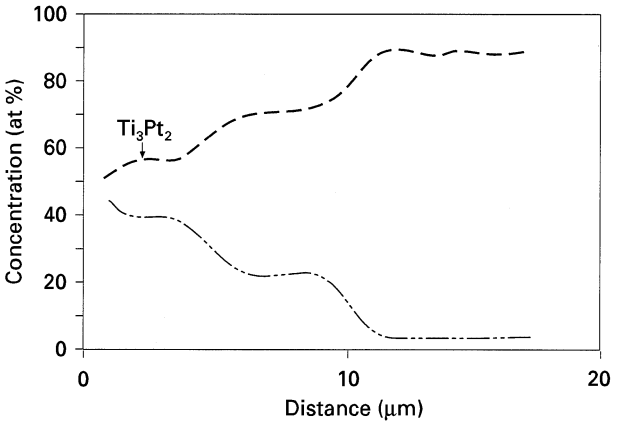

Figure 5 High-resolution EPMA profile (0.3 μm point to point) of a ZrO_2/Pt/Ti joint (1245 °C; 90 min) showing the "Ti_3Pt_2" plateau. (– – –), Ti; (— - - —), Pt.

Layer *g* has a duplex microstructure, not visible in the micrographs owing to contrast effects, whose mean composition corresponds to 5 at% Pt, 8 at% O and 87 at% Ti. This is due to the simultaneous formation of α-Ti(O) + Ti_3Pt, at temperatures lower than those of joining, from a mixture of near-binary eutectoid (3 at% Pt–97 at% Ti) composition.

The level of oxygen is systematically higher in layer *g* and in the Ti metal than in the intermetallics. This is related to the oxygen solubility in α-Ti and its presumably lower solubility in the intermetallics. If pick-up of residual oxygen from the argon atmosphere is not considered, the only source of oxygen is the ceramic. To confirm this hypothesis, asymmetric sandwiches ZrO_2/Pt/Ti/ZrO_2 fired at 1162 °C for 180 min were analysed for oxygen across the thickness of the titanium, and it was found that [O] increases progressively from about 10 at% on the Pt/Ti side (*g*/Ti interface) to about 20 at% on the Ti/ZrO_2 side, which is consistent with the asymmetry of the joints; if [O] in Ti were determined by residual atmospheric oxygen, one would expect an essentially uniform [O] across the metal. It is thus hypothesized that migration of Ti across the Pt foil towards the ceramic will result in a Pt(Ti) activated solid solution capable of decomposing the zirconia, the resultant oxygen being pumped away, through the intermetallics meanwhile formed, to the α-Ti phase.

In connection with the previous interpretation, it is noteworthy that the interface between the ceramic and the Pt-rich phase is rugged after joining. High magnifications (Fig. 6) show that this corresponds to a penetration of a Pt-rich phase along the grain boundaries of the ceramic, with dissolution of the latter, resulting in an intrusion of a liquid-like phase. Although platinum can form with sufficient amounts (greater than 60 at%) of zirconium metal a liquid phase at temperatures as low as 1200 °C [6], this penetration is not present in specially prepared ZrO_2–Pt joints. Thus, there must be some effect of dissolved titanium in promoting locally a possible liquid phase, presumably through a previous reaction with the ceramic.

3.2.2. Joints in the presence of a liquid phase

Joints made at 1328 and 1494 °C present an additional duplex layer *l* between *d* and *e* (Fig. 7), whose average composition is $Ti_{0.52}Zr_{0.03}Pt_{0.45}$ or, for practical purposes, $Ti_{0.55}Pt_{0.45}$. Most probably, it is formed by a mixture of the phases "Ti_3Pt_2" and TiPt and seems to result from the eutectic solidification of a liquid formed at joining temperatures. In the compositional range of interest for the discussion, the Ti–Pt binary presents an eutectic reaction at 1310 °C [5] but the eutectic composition (with 33 at% Pt) is far from the measured composition of *l*. Assuming that the phases formed during joining are not far from equilibrium (as suggested by the fact that their presence and

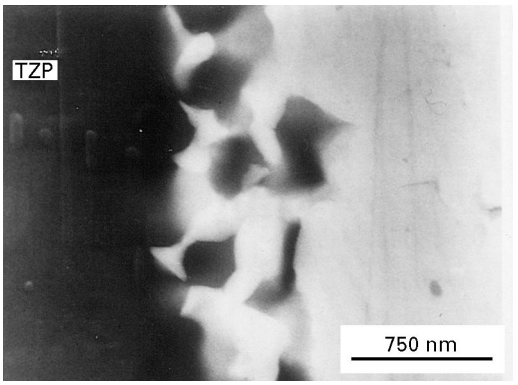

Figure 6 Penetration along ceramic grain boundaries in a ZrO_2/Pt/Ti joint (1162 °C; 180 min).

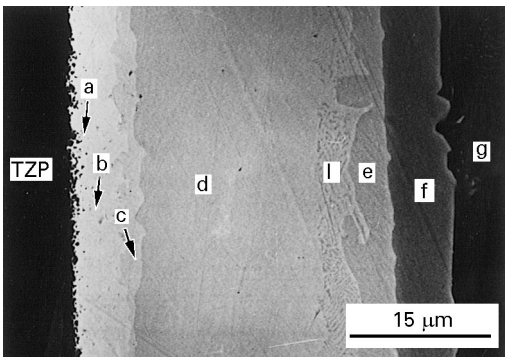

Figure 7 Microstructure of a ZrO_2/Pt/Ti joint with liquid-phase formation (1328 °C; 15 min).

composition are not significantly affected by joining temperature and time) and that the vestigial [Zr] and [O] do not produce dramatic effects in the phase relationships, the presence of *l* and *e* between Ti_3Pt and TiPt calls for a revision of the Pt–Ti phase diagram in this region. It is possible that instead of the Ti_3Pt + TiPt + L eutectic equilibrium so far proposed, another eutectic "Ti_3Pt_2" + TiPt + L compatibility relationship exists, with the liquid composition displaced towards the Ti-rich end of the TiPt phase (47 at% Pt). In this case the "Ti_3Pt_2" phase would result from a peritectic reaction between Ti_3Pt and liquid, at a temperature above the eutectic (Fig. 8).

At these higher temperatures, there is a merging of the *a* and *b* layers, to produce a virtually inextricable Pt- and Zr-rich layer, which becomes discontinuous with time, and reflects a strong interaction with the ceramic (Fig. 9). Also, for joining times greater than 15 min at 1328 °C and 1 min at 1494 °C, there is formation of an oxide layer c_{ox} between the (Pt, Zr)-rich layer and *d*. This layer can also assume a discontinuous character and thickens rapidly with time (at 1328 °C, 5 μm after 30 min, and 30 μm after 60 min). EDS analysis of oxygen and titanium in this oxide gave for its composition Ti_2O_3, other elements remaining undetected. This oxide is thought to form as the result of reaction of titanium-activated platinum with the ceramic, transport of oxygen across the Pt-rich layer and its reaction with the titanium. This may come from the *c* layer or may diffuse through the

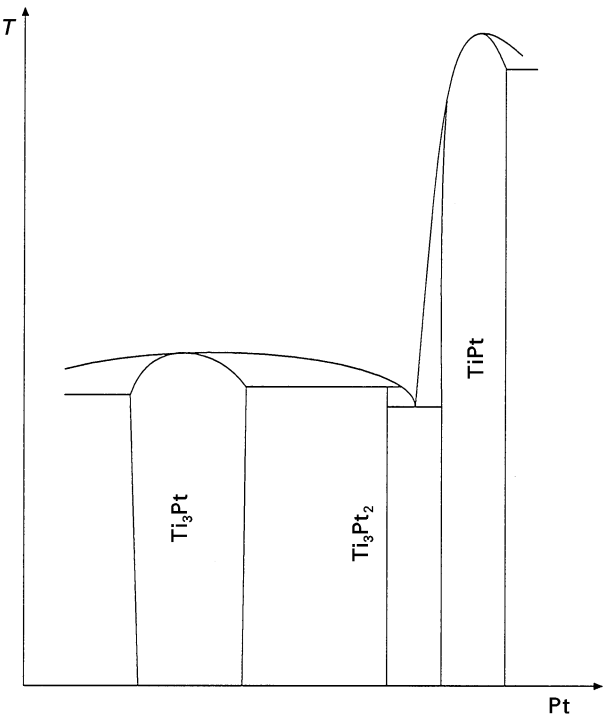

Figure 8 Schematic tentative Pt–Ti diagram describing phase relationships in the presence of "Ti_3Pt_2" (based on [5]).

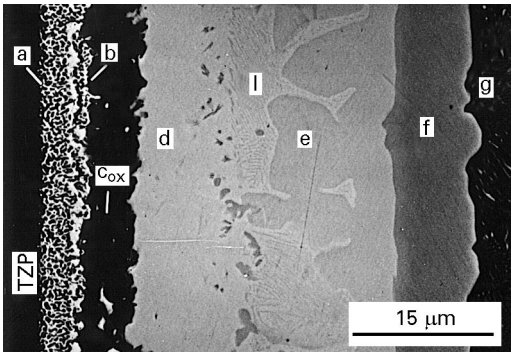

Figure 9 Microstructure of a ZrO_2/Pt/Ti joint with both liquid-phase and oxide layer formation (1328 °C; 30 min).

intermetallics. EPMA profiles show indeed an increase in [Zr] in the (Pt, Zr)-rich layer and an increase in [O] in layer *c*, even before c_{ox} starts to form.

The fracture strength of all the ZrO_2/Pt/Ti joints is rather low and seems to be conditioned by the strength of the ZrO_2–Pt-rich layer interface since all the fractures run along that interface. The presence of a presumably brittle Ti_2O_3 layer does not change this behaviour.

3.3. Tetragonal zirconia polycrystal/Pt/(Ti–6 wt% Al–4 wt% V) system

The main difference relative to the previous system is the formation of liquid *l* and of the oxide layer b_{ox}, now of nominal composition TiO, instead of Ti_2O_3, at lower temperatures. Liquid forms already at 1162 °C, whereas the oxide appears in joints made at 1245 °C after 90 min. The reason for the formation, in the

present system, of an oxide richer in Ti is not clear, but it is probably connected with higher kinetics for Ti diffusion promoted by low concentrations of Al and V, elements which also decrease the solidus temperature of the *l* layer. The layer sequence is otherwise similar to that in the ZrO_2/Pt/Ti system (Figs 10 and 11), apart from some details: (1) growth of phase *e* by coalescence with the same phase in the *l* microstructure; (2) a serrated *f*–*g* interface; (3) the presence of a relatively thick Ti-rich layer in *g*, adjacent to *f*. The presence of the latter was already detected in the TZP/Pt/Ti joints and interpreted as the expression of the equilibrium Ti solid solution + Ti_3Pt along a continuous interface, the same equilibrium that is present in the duplex structure which forms the bulk of *g*.

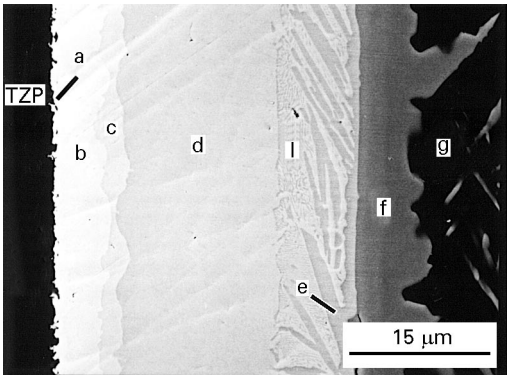

Figure 10 Microstructure of a ZrO_2/Pt/Ti6Al4V joint for short joining times (1328 °C; 15 min).

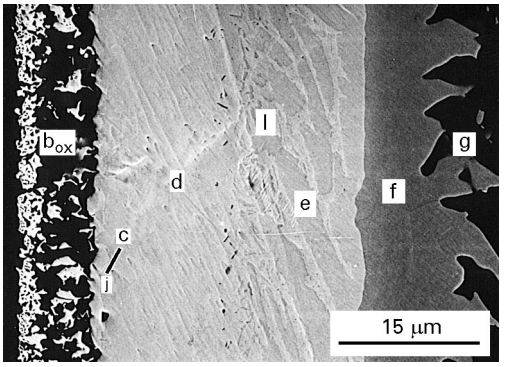

Figure 11 Microstructure of a ZrO_2/Pt/Ti6Al4V joint for longer joining times, showing a dark oxide layer (1328 °C; 30 min).

The compositional profile across an oxide-free joint is represented in Fig. 12, discarding the measurements for Al and V, for clarity; these measurements are below 5 at%, except in layer *g*, where they attain averages of 9 at% and 6 at%, respectively. It is seen that Ti migrates up to the Pt-rich layers (which are analytically indistinguishable) whereas the oxygen content is somewhat higher than in the previous system. It is likely that layers *c*, *d*, *e* and *f* are the same phases identified in the ZrO_2/Pt/Ti joints, allowance being made for vestigial amounts of V and Al. It is also evident that the analysis of the Ti-rich α, β-Ti(Al, V, O) portion occupying the first few micrometres of *g*, immediately adjacent to *f*, is virtually the same as in the duplex region, farther away from the *f*–*g* interface; this is consistent with the small amount of "Ti_3Pt" phase found in the duplex microstructure.

4. Conclusions

1. Direct ZrO_2–Ti joints have been obtained at 1328 and 1494 °C. The layer sequence in the joint was tentatively identified as $ZrO_{2-x}/(Zr,Ti)O_{2-x} + (Zr,Ti)_2O/(Zr,Ti)_2O/Ti[O]$. Ti metal is saturated with oxygen. The fracture path in those joints runs through the metal, which is embrittled by O intake and extensive grain growth.

2. Lower-temperature ZrO_2/Pt/Ti joints, where a Pt foil is inserted, present a complex sequence of interlayers that can mostly be described on the basis of the Pt–Ti binary.

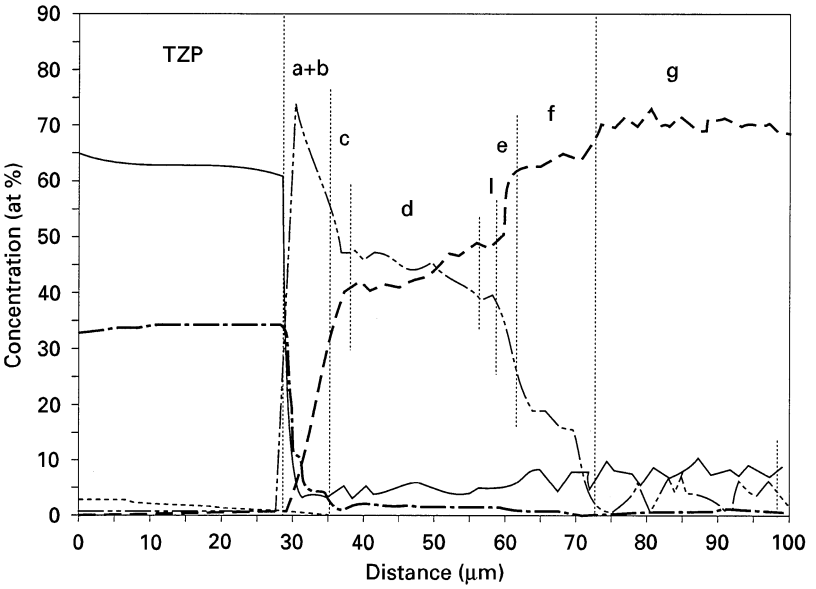

Figure 12 EPMA profiles in a ZrO_2/Pt/Ti6Al4V joint (the concentrations of Al and V, not shown, are less than 5 at% in all layers, except *g* (1328 °C; 15 min). (——), O; (– – –), Ti; (— - —), Zr; (— - - —), Pt; (- - - - -), Y.

3. Higher-temperature ZrO_2/Pt/Ti joints develop an oxide layer of composition Ti_2O_3, between a (Pt, Zr)-rich layer and the TiPt layer. It seems that oxygen resulting from a reaction of platinum (possibly activated by titanium) with the ceramic concentrates in this region to react with incoming titanium.

4. In all ZrO_2/Pt/Ti joints a phase of nominal composition "Ti_3Pt_2" forms. This phase is not predicted by the published Pt–Ti binary diagrams. It is proposed that this phase may establish an eutectic equilibrium with TiPt and a liquid of intermediate composition at a temperature near 1300 °C

5. The fracture path in ZrO_2/Pt/Ti joints runs through the interface between the ceramic and the (Pt, Zr) layer.

6. When Ti is replaced by Ti–6 wt% Al–4 wt% V, the main consequences are the presence of liquid at lower joining temperatures and the earlier development of an oxide layer of nominal composition TiO.

Acknowledgement

One of the authors (J. V. Emiliano) acknowledges a grant from Conselho Nacional de Desenvolvimento Científico e Tecnológico, Brazil.

References

1. J. V. EMILIANO, R. N. CORREIA, P. MORETTO and S. D. PETEVES, in Proceedings of the 7th International Conference on Intergranular and Interface Boundaries in Materials, Lisbon, June 1995, *Mater. Sci. Forum* **207**–**209**, part 1 pp. 145 (1996)
2. J. L. MURRAY, "ASM handbook", Vol. 3 "Alloy phase diagrams" (1992) p. 2.380.
3. J. L. MURRAY and H. A. WRIEDT, *ibid.* p. 2.324.
4. R. F. DOMAGALA, S. R. LYON and R. RUH, *J. Am. Ceram. Soc.* **56** (1973) 584.
5. J. L. MURRAY, "ASM handbook", Vol. 3, "Alloy phase diagrams" (1992) p. 2.348.
6. H. OKAMOTO, *ibid.* p. 2.349.

Received 23 April 1996
and accepted 30 July 1997